A Journal of the Gesellschaft Deutscher Chemiker
Angewandte
GDCh
International Edition
Chemie
www.angewandte.org

Accepted Article

Title: An interface bridged organic-inorganic layer suppressing dendrite and side reactions for ultra-long life aqueous Zn metal anodes

Authors: Yanhui Cui, Qinghe Zhao, Xiaojun Wu, Xin Chen, Yuetao Wang, Runzhi Qin, Shouxiang Ding, Yongli Song, Junwei Wu, Kai Yang, Zijian Wang, Zongwei Mei, Zhibo Song, Hong Wu, Zhongyi Jiang, Guoyu Qian, Luyi Yang, Feng Pan, and Jinlong Yang

This manuscript has been accepted after peer review and appears as an Accepted Article online prior to editing, proofing, and formal publication of the final Version of Record (VoR). This work is currently citable by using the Digital Object Identifier (DOI) given below. The VoR will be published online in Early View as soon as possible and may be different to this Accepted Article as a result of editing. Readers should obtain the VoR from the journal website shown below when it is published to ensure accuracy of information. The authors are responsible for the content of this Accepted Article.

To be cited as: *Angew. Chem. Int. Ed.* 10.1002/anie.202005472

Link to VoR: https://doi.org/10.1002/anie.202005472

WILEY-VCH

10.1002/anie.202005472

RESEARCH ARTICLE

WILEY-VCH

An interface bridged organic-inorganic layer suppressing dendrite and side reactions for ultra-long life aqueous Zn metal anodes

Yanhui Cui,[a] Qinghe Zhao,[a] Xiaojun Wu,[b] Xin Chen,[a] Jinlong Yang,[a][c]* Yuetao Wang,[a] Runzhi Qin,[a] Shouxiang Ding,[a] Yongli Song,[a] Junwei Wu,[d] Kai Yang,[a] Zijian Wang,[a] Zongwei Mei,[a] Zhibo Song,[a] Hong Wu,[e] Zhongyi Jiang,[e] Guoyu Qian,[a] Luyi Yang,[a]* and Feng Pan,[a]*

[a] Dr. Y. Cui, Dr. Q. Zhao, X. Chen, Y. Wang, Dr. R. Qin, S. Ding, Dr. Y. Song, K. Yang, Z. Wang, Dr. Z. Mei, Z. Song, Dr. G. Qian, Dr. L. Yang, Dr. J. Yang, Prof. F. Pan
School of Advanced Materials
Peking University Shenzhen Graduate School
Shenzhen 518055, PR China
E-mail: yangly@pkusz.edu.cn; yangjl@pkusz.edu.cn; panfeng@pkusz.edu.cn

[b] Dr. X. Wu
School of Chemical Biology and Biotechnology
Peking University Shenzhen Graduate School
Shenzhen 518055, PR China

[c] Dr. J. Yang
Department of Materials Science and Engineering
Stanford University
Stanford, CA, 94305, USA

[d] Dr. J. Wu
Department of Materials Science and Engineering
Harbin Institute of Technology (Shenzhen)
Shenzhen 518055, PR China

[e] Prof. H. Wu, Prof. Z. Jiang
Key Laboratory for Green Chemical Technology of Ministry of Education, School of Chemical Engineering and Technology
Tianjin University
Tianjin 300072, PR China

Supporting information for this article is given via a link at the end of the document.

Abstract: Aqueous zinc (Zn) batteries (AZBs) are widely considered as a promising candidate for next-generation energy storage owing to its excellent safety feature. However, the application of Zn anode is hindered by severe dendrite formation and side reactions. Herein an interfacial bridged organic-inorganic hybrid protection layer (Nafion-Zn-X) is developed by complexing inorganic Zn-X zeolite nanoparticles with Nafion, which shifts ion transport from channel transport in Nafion to hopping mechanism in organic-inorganic interface. This unique organic-inorganic structure is found to effectively suppress dendrite growth and side reactions of Zn anode. Consequently, Zn@Nafion-Zn-X composite anode delivers high coulombic efficiency (~97%), deep Zn plating/stripping (10 mAh cm^{-2}) and long cycle life (over 10000 cycles). By tackling the intrinsic chemical/electrochemical issues, the proposed strategy provides a versatile remedy for the limited cycle life of Zn anode.

Introduction

Lithium-ion batteries (LIBs) are widely used in electric vehicle and portable electronic applications for their outstanding electrochemical performances.[1-5] However, conventional LIBs suffer from safety issues due to the usage of flammable/explosive organic electrolytes.[6-7] Therefore, developing safer energy storage systems are urgently needed. Operated in non-flammable aqueous electrolyte, aqueous zinc batteries (AZBs) are considered a much safer alternative to LIBs.[8-12] In addition, AZBs also possess other advantages, including non-toxicity, low cost and minimum requirement for atmosphere.[13-14] In the last decade, most efforts are focused on enhancing battery performance (capacity delivery, cycling stability, or rate property) of cathode materials in AZBs, including active materials of manganese oxides, [15-17] vanadate compounds,[18] Prussian blue,[19] organic cathode,[20] and so on. However, Zn metal anode is also faced with critical challenges such as dendrite growth, and side reactions including hydrogen evolution reaction (HER) and byproduct (e.g. an inert $Zn_4(OH)_6SO_4 \cdot 5H_2O$ in $ZnSO_4$ aqueous electrolyte) formation (**Scheme 1a**), which generally lead to low coulombic efficiency, capacity fading and short/open circuit, thereby the commercialization of AZBs are severely hindered.[21]

This article is protected by copyright. All rights reserved.

Accepted Manuscript

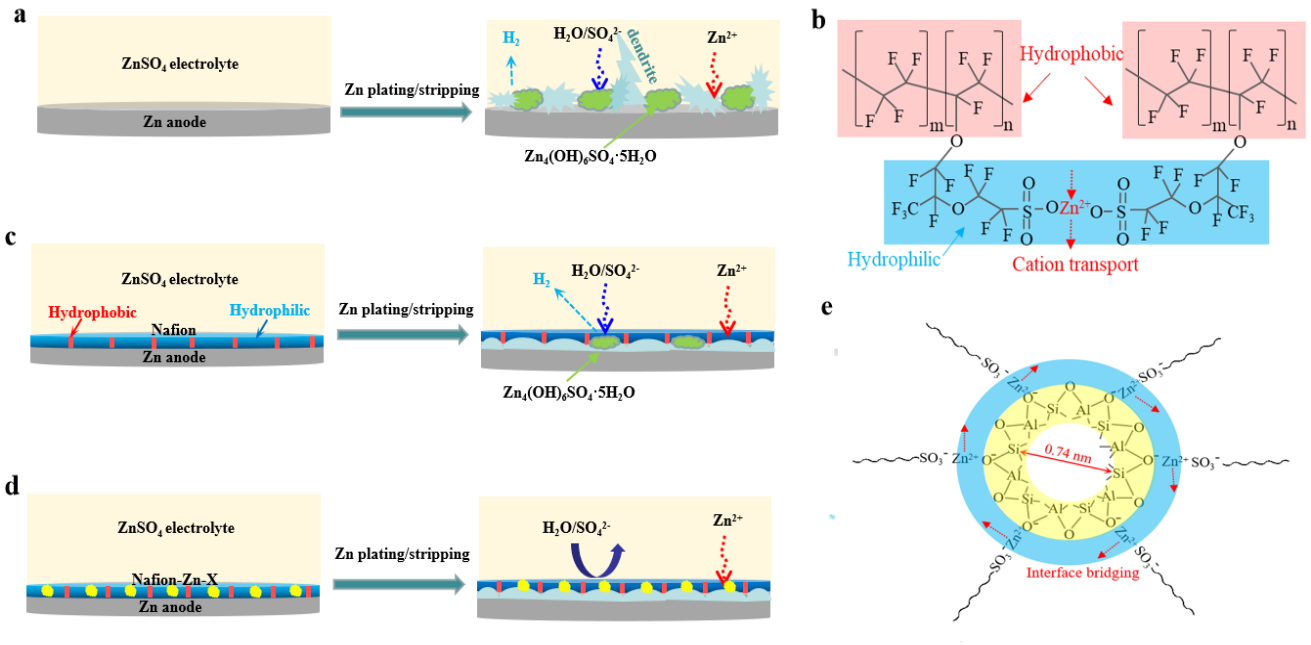

Scheme 1. (a) Schematic drawing of Zn cycling on bare Zn, (b) organic structure of Nafion with Zn^{2+}, protection effect comparison of (c) Zn@Nafion and (d) Zn@Nafion-Zn-X anode in aqueous Zn ion batteries; (e) proposed organic-inorganic interface of Nafion-Zn-X composites.

To address the above issues, the currently reported solutions can be divided into two aspects: suppressing dendrite formation and minimizing side reactions. Dendrite suppression can be achieved by introducing coating layers on Zn anode surface which effectively modified the current and electrolyte flux on anode surface, such as $CaCO_3$ and SiO_2 layer,[22] porous active carbon layer and reduced graphene oxide (rGO) layer,[23, 24] etc. In addition, many strategies have also been reported for relieving the side reactions beside suppressing dendrites, including coating a zincophilic protective layer,[25] replacing $ZnSO_4$ with $Zn(CF_3SO_3)_2$,[26] using electrolyte additives,[27-29] adoption of a highly concentrated zincic salt as electrolyte,[30] using modified conductive host,[31-34] employing single ion conductive electrolyte,[35, 36] alloying with Al,[37] adopting gel electrolyte or all solid electrolyte,[38-40] coating inorganic layer[41-44] or organic (polyamide) layer,[45] etc. Indeed, the side reactions and dendrite are very important issues for long life AZBs. However, the intrinsic mechanism of suppressing side reactions and dendrite were not demonstrated very clearly, and more experiments are still desirable for ensuring the influence factors, e.g. dynamic behavior and relationship of cations, anions and aqueous solution on Zn anode surface, etc.

In addition, the current reported protection strategies, including inorganic or organic coating layers, are limited in improving the performance and life of zinc anode. The inorganic one is brittle, which is easy to fracture after long-cycled or fast Zn plating/striping. The organic one is flexible, but a hydrophobic polymer layer causes an increase of polarization potential for Zn plating/stripping dramatically due to the elevated nucleation barrier and restricted 2D diffusion of Zn^{2+},[45] and an excessively hydrophilic polymer dissolves easily in the aqueous electrolyte, resulting in loss of protection against Zn anode. Nafion membrane, already used as a separator (thickness > 100 um) with selective cationic transport in aqueous cell,[46,47] is composed by hydrophilic and hydrophobic regions (Scheme 1b, protons of Nafion along with cycling will be replaced by Zn^{2+} gradually as shown in Figure S1), and seems to play an active role in Zn plating/stripping as well as dendrite protection. However, Nafion membrane (thickness $\leqslant$ 30 um, Figure S2) as the protection layer of Zn anode is unable to completely block other small molecules from passing through due to its internal 4 nm ion channels,[48] which may cause undesirable side reactions and compromise the coulombic efficiency (CE) of Zn plating/striping processes (Scheme 1c). Therefore, further modification of Nafion is very necessary to improve the performance of protective layer.

Herein we designed and synthesized an organic-inorganic composite (Nafion-Zn-X) protection layer by complexing Nafion with Zn-X zeolite (Scheme 1d). This composite protection layer, in which Zn-ion bridges the interface between Zn-X and Nafion, not only effectively shields anion and free H_2O to suppress side reactions, but also suppresses Zn dendrites by uniform Zn plating/stripping.

Results and Discussion

The composite protection layers were prepared using Nafion solution and Zn-X zeolite nanoparticles, which were stirred to form a slurry and recasted on the surface of Zn plate (detail procedure are shown in experimental section). To improve the protective effect of Nafion membrane on Zn plate, the structure of inorganic filler is very important. Zn-X zeolite (Scheme 1e, XRD, SEM and EDS results are shown in Figure S3 and Figure S4), firstly, is a (Si, O, Al) alternate frame structure with negative charge and coordinated with Zn cations, in which the maximal pore size is about 0.74 nm much smaller than channel size in Nafion (4 nm) [49], thus the cations(Zn^{2+}) can travel freely on the surface/inter surface of Zn-X by hopping mechanism (the Zn^{2+} conductivity is confirmed by EIS shown in Figure S5) while most

This article is protected by copyright. All rights reserved.

Accepted Manuscript

anions can be shielded. Furthermore, the synthesized Zn-X filler with nanoscale and has large BET surface area (Figure S6) which can dynamically cross-link with Zn-Nafion via Zn^{2+} (Scheme 1e) to form well-bridged compact organic-inorganic interfaces and restrain SO_4^{2-} to transport forward. The Fourier transform infrared spectra (FTIR) results (Figure S7) confirms the organic-inorganic interface is reconstructed by the bridge bond between sulfonate ($-SO_3^-$) of Nafion and Zn^{2+} on the surface of Zn-X zeolite. E.g. when Zn^{2+} replaces Na^+ and coordinates with (-Al-O^--Si-) framework in zeolite, two new peaks appear at 1572 and 1430 cm^{-1}, corresponding to Lewis and Brønsted acid sites, which are attributed to water decomposition caused by the enlarged distance between Zn^{2+} cation and ($-O^-$) anion site.[50-52] After combined with Nafion, Lewis and Brønsted acid peaks in Nafion-Zn-X re-disappear due to the re-coordination. However, this phenomenon did not appear in Zn-X covered with Nafion (Figure S8). The FTIR results demonstrate the Zn^{2+} in Zn-X is coordinated with ($-SO_3^-$) of Nafion. In addition, the shift of wave number in ($-SO_3^-$) site(Figure S7b), the change of binding energies at Zn2p, O1s and F1s (Figure S9) further prove the presence of (~SO_3^--Zn^{2+}~) bridge bond structure in Nafion-Zn-X composite as shown in Figure S10. It should be also noted that the hydrophilic Zn-X zeolite was merged into the hydrophilic region of Nafion membrane, thus the size of hydrophilic cavity is reduced to further suppress Zn dendrites and side reactions. Based on the properties above, we expect that such organic-inorganic protective coating would enhance the cycle life of Zn metal anodes in aqueous batteries.

To investigate protection effect of the organic-inorganic coating layers on Zn anode, we firstly coated pure Nafion and Nafion-Zn-X zeolite composite slurry on the surface of Cu current collector and then assembled three asymmetry cells (Cu¦Zn, Cu@Nafion¦Zn@Nafion and Cu@Nafion-Zn-X¦Zn@Nafion-Zn-X) to test the reversibility of Zn plating/striping. The side reaction levels of these anodes can be demonstrated by capacity retention after cycles.[53] Firstly, a reservoir capacity

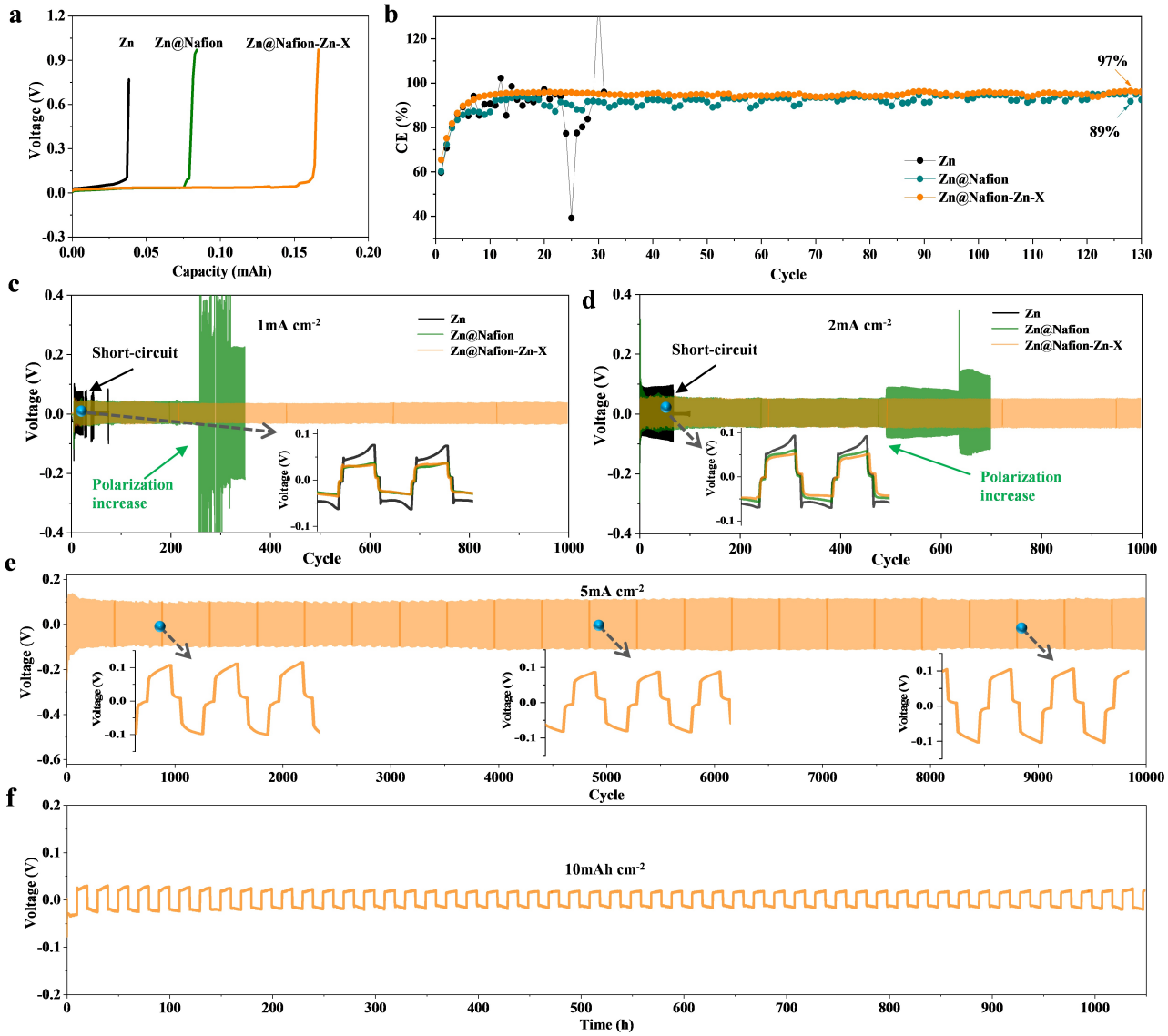

Figure 1. Electrochemical performances.(a, b) Cu¦Zn asymmetry cells to investigate the reversibility of Zn plating/striping: (a) voltage/capacity plots of Zn stripping from Cu electrode after 24 cycles, Cu@Nafion and Cu@Nafion-Zn-X electrodes after 50 cycles with an initial reservoir capacity of 2 mAh cm^{-2} and a constant current density of 0.2 mA cm^{-2}, (b) CE performances of Cu¦Zn, Cu@Nafion¦Zn@Nafion and Cu@Nafion-Zn-X¦Zn@Nafion-Zn-X cells with 0.5 mAh cm^{-2} plating and striping at 0.5 mA cm^{-2}; (c-f) Zn¦Zn symmetrical cells to investigate cycling performance of Zn, Zn@Nafion, Zn@Nafion-Zn-X anodes with area capacities of 0.5 mAh cm^{-2} and different current densities of (c) 1 mA cm^{-2}, (d) 2 mA cm^{-2}, (e) 5 mA cm^{-2}, (f) 10 mAh cm^{-2} and 1 mA cm^{-2}.

This article is protected by copyright. All rights reserved.

Accepted Manuscript

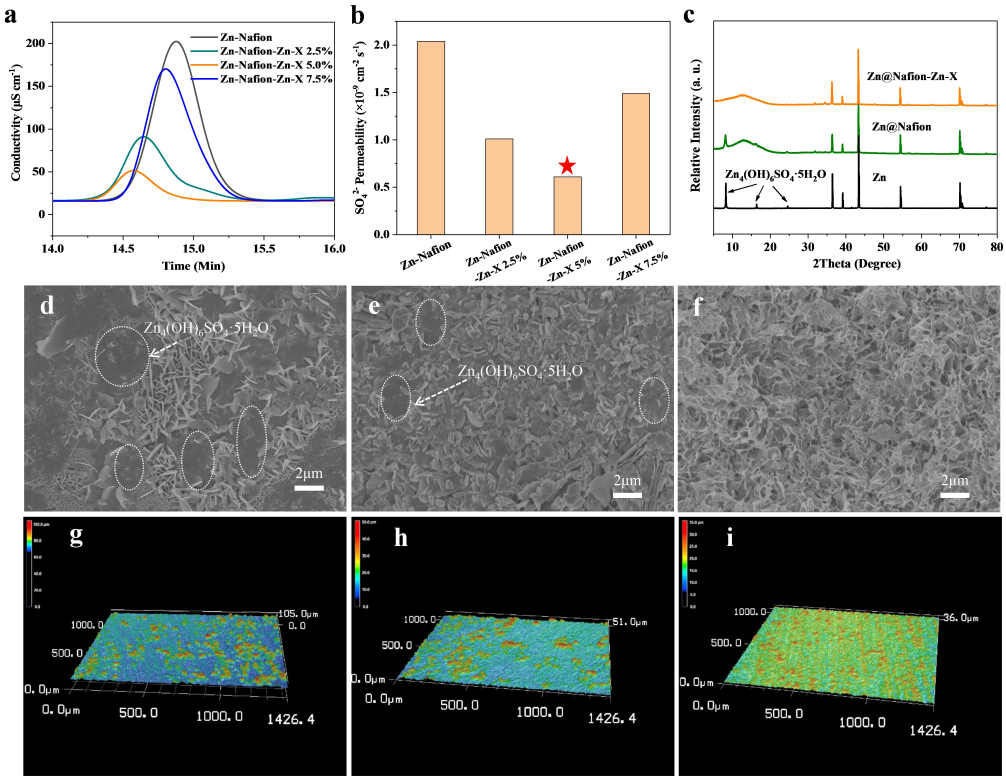

Figure 2. (a) Conductivity/time curves of $ZnSO_4$ concentration collected after 1 h permeability with different membranes; (b) SO_4^{2-} permeability of Nafion and Nafion-Zn-X composite membranes; (c) XRD patterns, (d-f) SEM and (g-i) CLSM optical images of (d, g) bare Zn, (e, h) Zn@Nafion, and (f, i) Zn@Nafion-Zn-X anodes after 1 h Zn plating process at 0.5 mA cm^{-2}.

of 2 mAh cm^{-2} was plated on both bare Cu and coated Cu electrodes at 0.2 mA cm^{-2}, then cycled 50 times with a capacity of 0.2 mAh cm^{-2} at 0.2 mA cm^{-2}, finally, the remaining Zn was stripped to 1 V at 0.2 mA cm^{-2}. It can be observed from **Figure 1a** (the corresponding voltage/time plots are shown in Figure S11) that the stripped Zn are 0.038 mAh at 24th cycle, 0.084 mAh at 50th cycle, and 0.166 mAh at 50th cycle for asymmetry batteries with no protective layer, Nafion layer and Nafion-Zn-X layer, respectively, indicating that Nafion-Zn-X later suppresses the side reaction significantly. In addition, the values of CE during long-term cycling are also measured, as shown in Figure 1b (the corresponding plating/striping curves are shown in Figure S12). The results show that the unprotected Zn electrode can only sustain 30 cycles, with the lowest CE of only 40%. The CEs of electrodes with protective layer are obviously improved. For Zn@Nafion electrode, the CE is fluctuating around 90%. More importantly, it should be noted that after initial several cycles the CE of Zn@Nafion-Zn-X¦Zn cell is stable at 97%, demonstrating well suppressed side reaction suppressions by Nafion-Zn-X layer.

To further verify the enhancing effect of the organic-inorganic coating layers, all Zn anodes including the bare Zn, Zn@Nafion, and Zn@Nafion-Zn-X are assembled and tested in symmetry cells, and the corresponding cycling performance are presented as Figure 1c-f and Figure S13. It can be observed that there are different failure mechanisms in Zn¦Zn symmetric cells. For the bare Zn anode, short-circuit induced failure occurs in a few cycles (~ 32 cycles at 1 mA cm^{-2} and ~ 71 cycles at 2 mA cm^{-2}), mainly due to the dendrite formation. While for Zn@Nafion anode, the polarization induced failure (a sudden increase of polarization voltages) occurs in about several hundreds of cycles (~ 252 cycles at 1 mA cm^{-2} and ~ 489 cycles at 2 mA cm^{-2}), which could be attributed to lots of side reactions which exhausts electrolyte almost. By contrast, Zn@Nafion-Zn-X anode exhibits much better cycling stability for over 1000 cycles. Especially, the cells using Zn@Nafion-Zn-X anode can operate over 10000 cycles even at a high current density of 5 mA cm^{-2} (0.5 mAh cm^{-2}) (Figure 1e), which surpasses most previously reported works (Table S1). Furthermore, the cells using Zn@Nafion-Zn-X anode can operate well (over 1000 h) with deep Zn plating/stripping (10 mAh cm^{-2}) (Figure 1f). These results proved that the Nafion-Zn-X composite coating has a very good protective effect on the Zn anode and can promote its long cycle life.

Meanwhile, it should be noted that the polarization voltage values (PVVs) of Zn¦Zn cells with Nafion-based coatings are much lower than that of bare Zn anode. E.g. at current density of 2 mA cm^{-2}, the PVVs of bare Zn is about 90 mV, respectively; however, the values of both Zn@Nafion and Zn@Nafion-Zn-X anodes are similar about 50 mV, respectively, indicating the depolarization effects of Nafion based coating layers. For further elaborating the function of Nafion, PVDF replaced Nafion to be coated on Zn anode mixing with Zn-X. The cycling curves (Figure S14) show a large overpotential of Zn plating/stripping and even open circuit can be observed. Therefore, the Nafion component in protective layer facilitates to decrease overpotential of Zn plating/stripping.

To further evaluate the practical applications of the Nafion-Zn-X coating layer, batteries with VS_2 and active carbon (AC) cathodes were assembled and tested. Figure S15 shows the VS_2/Zn battery with bare Zn failures only after 74 cycles, and serious dendrites form on the surface of Zn anode (Figure S16a and Figure S17). However, the VS_2 batteries with Nafion-Zn-X coating layers can operate 600 cycles, which is consistent with the relative smooth Zn surface (Figure S16b). It should be noted that the degraded capacity is irrespective of the anode, e.g. the fresh cathode delivers high discharge capacity when matched with the cycled anode (Figure S15). In addition, the VS_2¦Zn@Nafion-Zn-X battery delivers better rate performance than that of pristine Zn (Figure S18). The enhancing effect of Nafion-Zn-X coating layer can also be verified by the active carbon (AC)¦Zn capacitors (Figure S19-S20). These results are according with the results in Zn¦Zn symmetry batteries and indicate a promising future of Nafion-Zn-X coating layer in AZB applications.

This article is protected by copyright. All rights reserved.

Accepted Manuscript

Next, the permeability of Nafion (control sample) and Nafion-Zn-X protective layers were tested by H-cells (Figure S21) with 2 mol L^{-1} of $ZnSO_4$ solution in one side and pure H_2O in another side. After 1 h stirred, the sample in H_2O side was collected and analyzed by ion chromatography (IC) (**Figure 2a**). The calculated permeability of SO_4^{2-} are shown in Figure 2b and Table S2. The results show the SO_4^{2-} permeability value of Nafion is 2.04×10^{-9} cm^2 s^{-1}, and it is obvious that the addition of Zn-X zeolite can further decrease the SO_4^{2-} permeability comparing with the blank Nafion membrane. The lowest one is 0.61×10^{-9} cm^2 s^{-1} for Nafion-Zn-X (with 5 wt% Zn-X), which is less than 30% of blank Nafion. Therefore, we conclude the Nafion-Zn-X composite coating layer can effectively screen SO_4^{2-} anions and protect Zn anode.

To confirm the failure mechanism of the Zn batteries, we disassembled the batteries and observed the surface composition and structure of Zn anodes (Figure 2c-i). For the short-circuit failed bare Zn¦Zn cell (and VS_2¦Zn battery), XRD (Figure 2c) shows high-strength impurity peaks in addition to Zn metal peaks, which are attributed to $Zn_4(OH)_6SO_4{\cdot}5H_2O$ byproduct. SEM (Figure 2d) images show many byproducts are intermingled in the Zn dendrites. The con-focal laser scanning microscope (CLSM) in Figure 2g shows surface altitude intercept is 105 μm. These results demonstrate that it is a large number of side reactions and dendrites that cause the battery to fail; For polarization failed Zn@nafion¦Zn@nafion cell, we found that the electrolyte has almost dried up, and XRD (Figure 2c), SEM (Figure 2e) and CLSM (Figure 2h) of the zinc surface after removing Nafion layer show that the dendrites are inhibited but still produce $Zn_4(OH)_6SO_4{\cdot}5H_2O$ byproducts, so side reactions are the main cause of battery failure. For Zn@Nafion-Zn-X¦Zn@Nafion-Zn-X cell, it is lack of byproduct in XRD (Figure 2c) and SEM images (Figure 2e). Meanwhile, the Zn plating morphology is smoother, e.g. the value of altitude intercept (Figure 2i) is only 36 μm for Zn@Nafion-Zn-X. Therefore, the Nafion-Zn-X composite coating layer suppresses dendrite and side reaction and guarantees the long cycle life of Zn anode in aqueous batteries.

Next, we further elaborate the protection mechanism of Nafion based composite coating layer. In cells, Zn plating/stripping includes two consecutive steps: (1) Zn^{2+} transport from electrolyte to the surface of anode and (2) redox reaction of Zn^{2+}/Zn^0 on the surface of anode. For bare Zn anode, there is one interface between $ZnSO_4$ electrolyte and anode, the redox reaction is following:

Electrolye|Zn anode: $Zn(H_2O)_6^{2+} \rightarrow Zn^0 + 6H_2O$ (1)

For Zn anode with Nafion based protective layers, there are two interfaces: one is that between $ZnSO_4$ electrolyte and Nafion, the other is between Nafion and anode. Two reaction processes happen at two interfaces as following:

Electrolye|Nafion:

$Zn(H_2O)_6^{2+} \rightarrow R\text{-}SO_3^-[Zn(H_2O)_x]^{2+}\text{-}SO_3\text{-}R + (6\text{-}x)H_2O$ (2)

Nafion|Zn anode:

$R\text{-}SO_3^-[Zn(H_2O)_x]^{2+}\text{-}SO_3\text{-}R \rightarrow Zn^0 + xH_2O$ $(1 \leqslant x \leqslant 4)$ (3)

To investigate the rate-determining step of Zn plating/stripping process (which could be Zn^{2+} transport or redox reaction), we compared the polarization curves of three Zn symmetric cells with $ZnSO_4$ electrolyte, (Zn-Nafion + $ZnSO_4$) electrolyte, and Zn-Nafion electrolyte (Figure S22). Compared with that of pure $ZnSO_4$ electrolyte both cells with Zn-Nafion added electrolyte

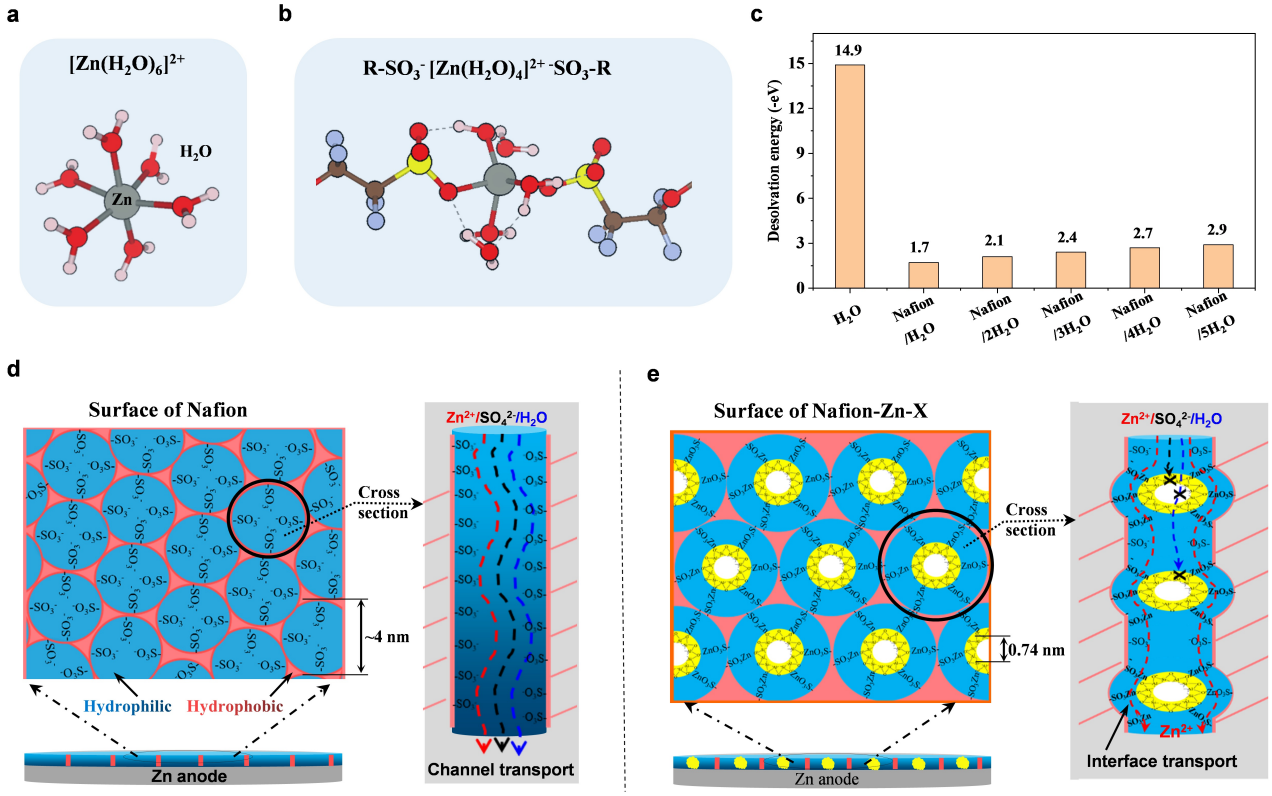

Figure 3. Protection mechanism of Nafion based layers. (a) Coordination environment of Zn^{2+} in water; (b) coordination environment of Zn^{2+} in Nafion with $4H_2O$; (c) desolvation energy values of Zn^{2+} in water or in Nafion with various H_2O (Gray-Zn, Yellow-S, Red-O, Pink-H, Blue-F, Brown-C); (d,e) Ion transport mechanisms in (d) Nafion and (e) Nafion-Zn-X protective layers.

This article is protected by copyright. All rights reserved.

Accepted Manuscript

have the same lower overpotential due to the same rate-determining step according the above redox reaction (3). Meanwhile, observing from the compared polarization curves of Zn plating/stripping (inset of Figure 1c and 1d), the overpotentials of Zn anode with Nafion based protective layer are significantly less than that of bare Zn anode. Therefore, the Nafion based layers can reduce the polarization of Zn^{2+}/Zn redox process.

Recently, Nazar proposed desolvation of Zn^{2+} should be consideration.[57] Here the desolvation energy barriers of Zn^{2+} are studied by Density Functional Theory (DFT) calculations (Figure 3a-c). In $ZnSO_4$ electrolyte, each Zn^{2+} is coordinated with six H_2O molecules, which delivers a high desolvation energy of Zn^{2+} (-14.9 eV/atom, Figure 3c). Whereas in Nafion-based layers, Zn^{2+} firstly can be coordinated with two R-SO_3^- which are linked on the backbone structure of Nafion, and then can be coordinated with H_2O molecules. The DFT results show Zn^{2+} is coordinated with $4H_2O$ molecules maximally (Figure 3b), which deliver desolvation energies of -2.4 eV/atom. By applying Nafion-based layers, the desolvation energies of Zn^{2+} (-1.7 ~ -2.9 eV/atom) with different H_2O molecules (Figure 3c) are much lower than that in water (-14.9 eV/atom). The lower desolvation energies facilitate to improve the kinetics of Zn plating/stripping and make its growth uniform to ensure its high rate performance and long cycle life.

In addition, water diffuses differently on the surface of zinc with or without Nafion protective layer. The electrolyte diffusion experiments in aqueous separator and Nafion membranes are shown in Figure S23. Observing that many water drops can flow out of the separator but they don't seem to be able to freely pass through the nafion protective membrane. The reason is due to Nafion is composed by hydrophilic and hydrophobic regions, and water molecules can only transport via the hydrophilic channels of ~ 4 nm (Figure 3d), and the domain-limited contact of electrolyte and metal anode is beneficial to suppress dendrite growth,[58] which are confirmed by the shorter surface altitude intercept (51 μm) on the Zn surface with protective layer compared with that on the bare Zn surface (105 μm). In brief, the roles of Nafion include the domain-limited contact of electrolyte and Zn anode to suppress dendrite growth and the reducing overpotentials of Zn plating/stripping to alleviate water decomposition to some extent.

However, pure Nafion layer is unable to completely block small anions (SO_4^{2-}) and free H_2O from passing through due to its internal hydrophilic channels, and the failure of the battery with Zn@Nafion anode is caused by the consumption of electrolyte due to side reactions involved other small molecules including SO_4^{2-}, H_2O and OH^-. Commonly, there are two main side reactions on Zn/electrolyte interface in the presence of $ZnSO_4$ electrolyte [36]:

$$\text{HER: } 2H_2O + 2e^- \rightarrow H_2\uparrow + 2OH^- \quad (4)$$

$$4Zn^{2+} + SO_4^{2-} + 6OH^- + 5H_2O \rightarrow Zn_4(OH)_6SO_4\cdot 5H_2O\downarrow \quad (5)$$

The reaction (5) shows it takes eleven H_2O molecules to form one $Zn_4(OH)_6SO_4\cdot 5H_2O$ formula on the surface of anode, including five crystalline H_2O and six OH^-. The consumption of OH^- will make the HER equilibrium shift to the right. In addition, many OH^- consumption decreases the pH value of electrolyte near anode which facilitates H_2 evolution.[10] However, after adding Zn-X, the hydrophilic channels were blocked by Zn-X particles as shown in Figure 3e. Due to the interfacial bridging between zeolite and sulfonic acid groups, compact interface was formed between Zn-X zeolite and Nafion in the hydrophilic channels. Due to negatively charged framework and small pore size of Zn-X zeolite, Zn^{2+} is allowed to hop along with the organic-inorganic interface while the other anions and free H_2O can be blocked, resulting in the suppression of side reactions including reaction (4) and (5). In addition, the calculated results from EIS experiments (Figure S5) show an increase in Zn^{2+} conductivity from 4.34 mS cm^{-1} of pure Nafion protective layer to 6.13 mS cm^{-1} of organic-inorganic composite Nafion-Zn-X layer, demonstrating the advantage of zinc ions transport at this organic and inorganic interfaces. Furthermore, it should be noted that more Zn-X in hybrid membrane is not always better, because zeolite segregation will arise when Zn-X addition is excessive, which will result in poorly arranged interfaces between Zn-X and Nafion.[54-56]

Conclusion

In this work, ion transport on Zn metal anode is regulated by an interfacial bridged hybrid protection layer consisting of Zn-X zeolite and Nafion, which serves as a barrier of small molecules except the Zn^{2+}. As a result, this protective layer decreases the side reactions significantly as well as Zn dendrite on the surface of Zn anodes. As a result, the Zn¦Zn symmetry batteries using Zn@Nafion-Zn-X anodes can well operate over 10000 cycles at a very high current density of 5 mA cm^{-2} as well as high areal capacity of 10 mAh cm^{-2}. The practical applications of Zn@Nafion-Zn-X are also verified by VS_2/Zn battery and C/Zn capacitor. This work demonstrates changing ion transport mechanism can be an effective strategy to suppressing open circuit and short circuit of AZBs and the proposed method provides a fresh perspective for developing long life AZBs.

(Detail experimental sections and supplementary characterization results are available in Supporting Information.)

Acknowledgements

Yanhui Cui, Qinghe Zhao and Xiaojun Wu contributed equally to this work. This work was financially supported by National Natural Science Foundation of China (No. 51602009), International Postdoctoral Exchange Fellowship Program (No. 20170098), National Key R&D Program of China (2016YFB070060), Soft Science Research Project of Guangdong Province (No. 2017B030301013), Shenzhen Science and Technology Research Grant (ZDSYS201707281026184), and China Postdoctoral Science Foundation (2019M650296).

Keywords: aqueous zinc anode • dendrite • SO_4^{2-} permeability • Nafion • Zn-X zeolite

[1] G. Zubi, R. Dufo-López, M. Carvalho, G. Pasaoglu, *Renew. Sustain. Energy Rev.* **2018**, *89*, 292-308.

[2] G. Qian, X. Liao, Y. Zhu, F. Pan, X. Chen, Y. Yang, *ACS Energy Lett.* **2019**, *4*, 690-701.

This article is protected by copyright. All rights reserved.

Accepted Manuscript

[3] R. Wang, G. Qian, T. Liu, M. Li, J. Liu, B. Zhang, W. Zhu, S. Li, W. Zhao, W. Yang, X. Ma, Z. Fu, Y. Liu, J. Yang, L. Jin, Y. Xiao, F. Pan, *Nano Energy* **2019**, *62*, 709-717.

[4] Y. Cui, Q. Zhang, J. Wu, X. Liang, A. P. Baker, D. Qu, H. Zhang, H. Zhang, X. Zhang, *J. Power Sources* **2018**, *378*, 40-47.

[5] Y. Cui, X. Wu, J. Wu, J. Zeng, A. P. Baker, F. Lu, X. Liang, J. Ouyang, J. Huang, X. Liu, Z. Li, X. Zhang, *Energy Storage Mater.* **2017**, *9*, 1-10.

[6] P. G. Balakrishnan, R. Ramesh, T. P. Kumar, *J. Power Sources* **2006**, *155*, 401-414.

[7] D. Lisbona, T. Snee, *Process Saf. Environ. Protect.* **2011**, *89*, 434-442.

[8] H. Li, L. Ma, C. Han, Z. Wang, Z. Liu, Z. Tang, C. Zhi, *Nano Energy* **2019**, *62*, 550-587.

[9] D. Yang, H. Tan, X. Rui, Y. Yu, *Electrochem. Energy Rev.* **2019**, 1-33.

[10] A. Konarov, N. Voronina, J. H. Jo, Z. Bakenov, Y. K. Sun, S. T. Myung, *ACS Energy Lett.* **2018**, *3*, 2620-2640.

[11] J. Long, J. Gu, Z. Yang, J. Mao, J. Hao, Z. Chen, Z. Guo, *J. Mater. Chem. A* **2019**, *7*, 17854-17866.

[12] J. F. Parker, J. S. Ko, D. R. Rolison, J. W. Long, *Joule* **2018**, *2*, 2519-2527.

[13] M. Song, H. Tan, D. Chao, H. J. Fan, *Adv. Funct. Mater.* **2018**, *28*, 1.

[14] X. Zeng, J. Hao, Z. Wang, J. Mao, Z. Guo, *Energy Storage Mater.* **2019**, *20*, 410-437.

[15] M. Liu, Q. Zhao, H. Liu, J. Yang, X. Chen, L. Yang, Y. Cui, W. Huang, W. Zhao, A. Song, Y. Wang, S. Ding, Y. Song, G. Qian, H. Chen, F. Pan, *Nano Energy* **2019**, *64*, 103942.

[16] Q. Zhao, S. Ding, A. Song, R. Qin, F. Pan, *Chinese J. Struct. Chem.* **2020**, 39, 388-394.

[17] W. Li, C. Han, Y. Wang, H. Liu, *Chinese J. Struct. Chem.* **2020**, 39, 31-35.

[18] B. Wu, G. Zhang, M. Yan, T. Xiong, P. He, L. He, X. Xu, L. Mai, *Small* **2018**, *14*, 1703850.

[19] W. Li, K. Wang, S. Cheng, K. Jiang, *Energy Storage Mater.* **2018**, *15*, 14-21.

[20] Z. Tie, L. Liu, S. Deng, D. Zhao, Z. Niu, *Angew. Chem. Int. Edit.* **2020**, 59, 4920-4924.

[21] B. Tang, L. Shan, S. Liang, J. Zhou, *Energy Environ. Sci.* **2019**, *12*, 3288-3304.

[22] L. Kang, M. Cui, F. Jiang, Y. Gao, H. Luo, J. Liu, W. Liang, C. Zhi, *Adv. Energy Mater.* **2018**, *8*, 1801090.

[23] W. Li, K. Wang, M. Zhou, H. Zhan, S. Cheng, K. Jiang, *ACS Appl. Mater. Interfaces* **2018**, *10*, 22059-22066.

[24] C. Shen, X. Li, N. Li, K. Xie, J. G. Wang, X. Liu, B. Wei, *ACS Appl. Mater. Interfaces* **2018**, *10*, 25446-25453.

[25] M. Liu, L. Yang, H. Liu, A. Amine, Q. Zhao, Y. Song, J. Yang, K. Wang, F. Pan, *ACS Appl. Mater. Interfaces* **2019**, *11*, 32046-32051.

[26] N. Zhang, F. Cheng, Y. Liu, Q. Zhao, K. Lei, C. Chen, X. Liu, J. Chen, *J. Am. Chem. Soc.* **2016**, *138*, 12894-12901.

[27] K. E. K. Sun, T. K. A. Hoang, T. N. L. Doan, Y. Yu, X. Zhu, Y. Tian, P. Chen, *ACS Appl. Mater. Interfaces* **2017**, *9*, 9681-9687.

[28] J. Hao, J. Long, B. Li, X. Li, S. Zhang, F. Yang, X. Zeng, Z. Yang, W. K. Pang, Z. Guo, *Adv. Funct. Mater.* **2019**, *29*, 1903605.

[29] Q. Zhang, J. Luan, L. Fu, S. Wu, Y. Tang, X. Ji, H. Wang, *Angew. Chem. Int. Edit.* **2019**, 58, 15841-15847.

[30] F. Wang, O. Borodin, T. Gao, X. Fan, W. Sun, F. Han, A. Faraone, J. A. Dura, K. Xu, C. Wang, *Nat. Mater.* **2018**, *17*, 543-549.

[31] Z. Wang, J. Huang, Z. Guo, X. Dong, Y. Liu, Y. Wang, Y. Xia, *Joule* **2019**, *3*, 1289-1300.

[32] R. Yuksel, O. Buyukcakir, W. K. Seong, R. S. Ruoff, *Adv. Energy Mater.* **2020**, 10, 1904215.

[33] Y. Yin, S. Wang, Q. Zhang, Y. Song, N. Chang, Y. Pan, H. Zhang, X. Li, *Adv. Mater.* **2020**, 32, 1906803.

[34] Y. Tian, Y. An, C. Wei, B. Xi, S. Xiong, J. Feng, Y. Qian, *ACS Nano* **2019**, 13, 11676-11685.

[35] Z. Wang, J. Hu, L. Han, Z. Wang, H. Wang, Q. Zhao, J. Liu, F. Pan, *Nano Energy* **2019**, *56*, 92-99.

[36] Y. Cui, Q. Zhao, X. Wu, Z. Wang, R. Qin, Y. Wang, M. Liu, Y. Song, G. Qian, Z. Song, L. Yang, F. Pan, *Energy Storage Mater.* **2020**, *27*, 1-8.

[37] S. B. Wang, Q. Ran, R. Q. Yao, H. Shi, Z. Wen, M. Zhao, X. Y. Lang, Q. Jiang, *Nature Commun.* **2020**, 11, 1-9.

[38] K. Leng, G. Li, J. Guo, X. Zhang, A. Wang, X. Liu, J. Luo, *Adv. Funct. Mater.* **2020**, 2001317.

[39] Y. Tang, C. Liu, H. Zhu, X. Xie, J. Gao, C. Deng, M. Han, S. Liang, J. Zhou, *Energy Storage Mater.* **2020**, 27, 109-116.

[40] L. Ma, S. Chen, N. Li, Z. Liu, Z. Tang, J. A. Zapien, S. Chen, J. Fan, C. Zhi, *Adv. Mater.* **2020**, 32, 1908121.

[41] X. Xie, S. Liang, J. Gao, S. Guo, J. Guo, C. Wang, G. Xu, X. Wu, G. Chen, J. Zhou, *Energy Environ. Sci.* **2020**, 13, 503-510.

[42] H. Yang, Z. Chang, Y. Qiao, H. Deng, X. Mu, P. He, H. Zhou, *Angew. Chem. Int. Edit.* **2020**, 59, 1-6.

[43] C. Deng, X. Xie, J. Han, Y. Tang, J. Gao, C. Liu, X. Shi, J. Zhou, S. Liang, *Adv. Funct. Mater.* **2020**, 2000599.

[44] H. He, H. Tong, X. Song, X. Song, J. Liu, *J. Mater. Chem. A* **2020**, 8, 7836-7846.

[45] Z. Zhao, J. Zhao, Z. Hu, J. Li, J. Li, Y. Zhang, C. Wang, G. Cui, *Energy Environ. Sci.* **2019**, *12*, 1938-1949.

[46] M. Ghosh, V. Vijayakumar, B. Anothumakkool, S. Kurungot, *ACS Sustainable Chem. Eng.* **2020**.

[47] M. Ghosh, V. Vijayakumar, S. Kurungot, *Energy Technol.* **2019**, *7*, 1900442.

[48] T. D. Gierke, G. E. Munn, F. C. Wilson, *J, Polym. Sci. Pol. Phys.* **1981**, *19*,1687-1704.

[49] R. L. V. Mao, E. Rutinduka, C. Detellier, P. Gougay, V. Hascoet, S. Tavakoliyan, S. V. Hoa, T. Matsuura, *J. Mater. Chem.* **1999**, *9*, 783-788.

[50] J.B. Uytterhoeven, R. Schoonheydt, B.V. Liengme, W. Keith Hall, *J. Catal.* **1969**, *13*, 425-434.

[51] V.B. Kazansky, I.R. Subbotina, N. Rane, R.A. Van Santen, E.J.M. Hensen, *Phys. Chem. Chem. Phys.* **2005**, *7*, 3088-3092.

[52] L. Wang, S. Sang, S. Meng, Y. Zhang, Y. Qi, Z. Liu, *Mater. Lett.* **2007**, *61*, 1675-1678.

[53] B. D. Adams, J. Zheng, X. Ren, W. Xu, J. G. Zhang, *Adv. Energy Mater.* **2018**, *8*, 1702097.

[54] Y. Cui, Y. Liu, J. Wu, F. Zhang, A. P. Baker, M. Lavorgna, Q. Wu, Q. Tang, J. Lu, Z. Xiao, X. Liu, *J. Power Sources* **2018**, *403*, 118-126.

[55] V. Di Noto, M. Piga, G. A. Giffin, K. Vezzù, T. A. Zawodzinski, *J. Am. Chem. Soc.* **2012**, *134*, 19099-19107.

[56] Y. Cui, A. P. Baker, X. Xu, Y. Xiang, L. Wang, M. Lavorgna, J. Wu, *J. Power Sources* **2015**, *294*, 369-376.

[57] E. Blanc, D. Kundu, L. F. Nazar, *Joule* **2020**, 4, 771-799.

[58] J. Wan, J. Xie, X. Kong, Z. Liu, K. Liu, F. Shi, A. Pei, H. Chen, W. Chen, J. Chen, X. Zhang, L. Zong, J. Wang, L. Q. Chen, J. Qin, .Y. Cui, *Nat. Nanotechnol.* **2019**, 14, 705-711.

Accepted Manuscript

This article is protected by copyright. All rights reserved.

10.1002/anie.202005472

Entry for the Table of Contents

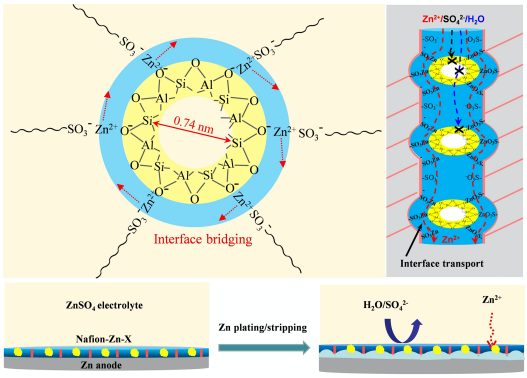

An interfacial bridged organic-inorganic (Nafion-Zn-X) protection layer is developed by complexing inorganic Zn-X zeolite nanoparticles with Nafion, which shift the ion transport from channel transport (Nafion) to hopping transport in organic-inorganic interface. This unique organic-inorganic structure suppresses dendrite and side reactions to guarantee the long cycle life of Zn anode in aqueous batteries.

WILEY-VCH
Accepted Manuscript

This article is protected by copyright. All rights reserved.